

# HR Diagrams of The Beehive Cluster (M44) and The Great Cluster in Hercules (M13)

June 13, 2023

## 1 Abstract

This paper details the process of imaging and plotting Hertzsprung-Russell (HR) diagrams for the Beehive Cluster (M44) and the Great Cluster in Hercules (M13). HR diagrams plot a star's color index against its absolute magnitude and are useful for determining a star cluster's age and stellar evolution. This project highlights the primary differences between open clusters and globular clusters: age and density. It also includes an analysis (and error analysis) of the signal to noise ratio values of several stars in each cluster. Finally, it discusses the significance of the results as it relates to previously observed trends in star clusters and presents suggestions for improvement and future projects.

## 2 Introduction

### 2.1 Theory

Hertzsprung-Russell (HR) diagrams (Figure 1) plot a star's luminosity as a function of its surface temperature (which is also directly related to its color.) HR diagrams are most useful for mapping a star's lifespan, which differs depending on its mass. Stars spend most of their lives on the main sequence (the diagonal line running from top left to bottom right), beginning their lives as hot, luminous, blue stars and gradually becoming cooler, less

luminous, and redder. Red giants and supergiants occupy the top right corner, and white dwarfs occupy the bottom left of the graph (*Hertzsprung-Russell Diagram*, n.d.-a). HR diagrams of star clusters reveal their ages via the Main Sequence Turn-Off. The point on the diagram in which the stars begin to move off the main sequence and toward the red giants marks the end of their life. Therefore, the main sequence lifetime of stars is the age of the cluster. Finding the age of star clusters is important on a larger scale because it confirms that there are no celestial objects older than the Big Bang, thus providing further support for the Big Bang Theory (Palma, n.d.).

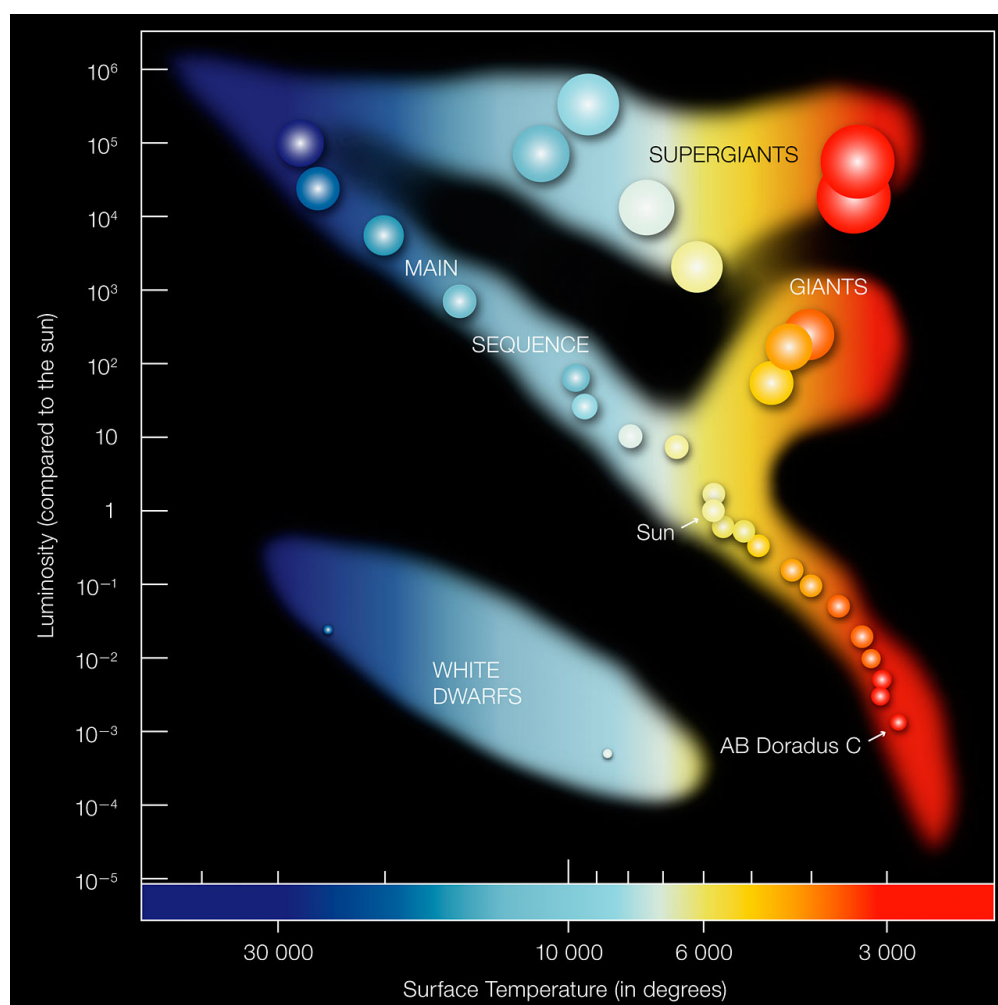


Figure 1: HR Diagram. Different classifications of stars fall on different areas on the plot. The turn-off point on this particular diagram is located at approximately (6000, 1), near our sun. (*Hertzsprung-Russell Diagram*, 2007)

M44, also known as the Beehive Cluster, is an open star cluster 600 light-years from Earth. It contains approximately 1000 stars and spans 15 light-years across. It occupies 1.5 degrees (or about 3 full moons, for reference) in the night sky, and it is visible as a faint cloud with the naked eye, although a telescope is required to see individual stars. At 600 million years old, it is a relatively young star cluster, so most of its stars are bright blue main sequence stars (Bolles, 2022).

M13, also known as the Great Cluster in Hercules, is a globular cluster 25,000 light-years from Earth. It contains approximately 100,000 stars and spans 150 light-years across. The stars in M13 are very densely packed (Leach & Block, 2008), and mostly red giants due to the cluster's old age (11.65 billion years) (Miller, 2017).



Figure 2: The Beehive Cluster (M44) (Evans, 2022)



Figure 3: The Great Cluster in Hercules (M13) (Leach & Block, 2008)

The primary differences between these clusters are their ages and whether or not they are gravitationally bound, which are connected properties. Open clusters (such as M44) contain younger stars that are not gravitationally bound to one another, while globular clusters (such as M13) contain older stars that are gravitationally bound. This is because open clusters form in the thick part of the galactic nucleus, which is densely packed with stars and other objects. These objects pull the cluster's stars away from each other and eventually disperse them. Therefore, any open cluster that has not been completely dispersed is young (less

than 1 billion years old in the Milky Way). Globular clusters, however, have a much longer lifespan than open clusters and can be much older. A globular cluster’s age is determined by its metallicity: older clusters have lower abundances of heavier elements because they formed before supernovae had dispersed heavier elements throughout the Universe. Despite the clusters themselves being very old, the Hubble Space Telescope and other observatories recently found that globular clusters contain multiple generations of stars (*Star Clusters*, n.d.).

We chose to analyze M13 and M44 due to their high visibility from Las Cumbres Observatory at this time of year (see Figures 4 and 5) and to compare and contrast HR diagrams of open and globular clusters.

## 2.2 Historical Background

Hertzsprung-Russell diagrams arose from the independent work of Ejnar Hertzsprung and Henry Norris Russell. Hertzsprung plotted the absolute magnitude of stars as a function of their color in 1911, while Russell plotted the absolute magnitude of spectral classes in 1913. They combined their work to find a relationship between luminosity and temperature (*The Hertzsprung-Russell Diagram*, n.d.-b).

M44 was first officially discovered by Galileo in 1609, though it was described as a manger in Greek and Roman mythology. It was later added to Messier’s catalog in 1769 (McClure & Byrd, 2023). M13 was discovered by Edmund Halley in 1714 and added to the Messier catalog in 1764, although Messier was “sure it doesn’t contain any star.” Sir William Herschel eventually discovered stars within M13 (Plotner, n.d.).

## 2.3 Importance

Although different, open and globular clusters each provide important information about our Universe. Open clusters, containing young stars, allow us to analyze stellar evolution. They also allow “main sequence mapping,” a method that involves using the common age and varying mass of the stars in a cluster to determine apparent brightness and luminosity to

ultimately find the cluster’s distance. Globular clusters are important because they contain stars that formed before the Milky Way’s disk, allowing us to study our galaxy’s history.

## 3 Methods

### 3.1 Imaging

We chose to analyze M44 and M13 due to their visibility from Las Cumbres Observatory in April and May. Las Cumbres Observatory’s visibility tool uses the right ascension and declination of an observation target to show the visibility of the target from each of their six global telescopes during a specified date range. As seen in Figures 4 and 5, M44 was visible for up to three hours at a time from all six telescopes, and M13 was visible for seven hours at a time from four telescopes.

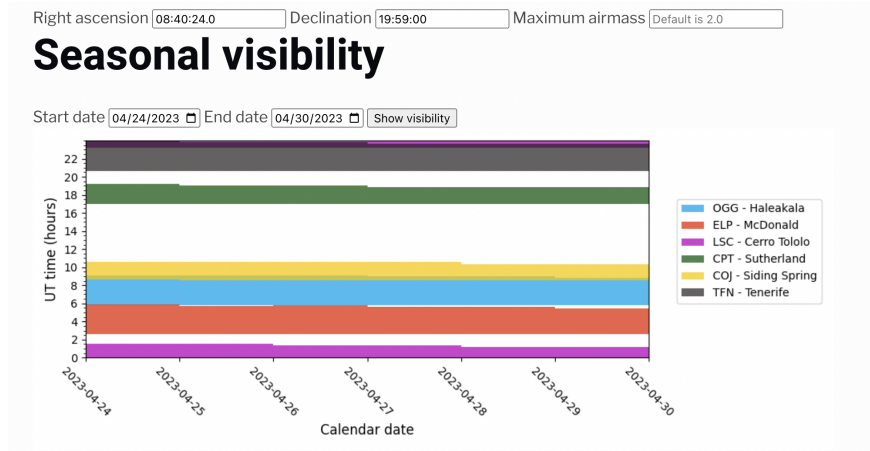


Figure 4: M44 visibility table. The colored lines represent the visibility at a given time from each telescope with the telescope of the corresponding color in the legend on the right.

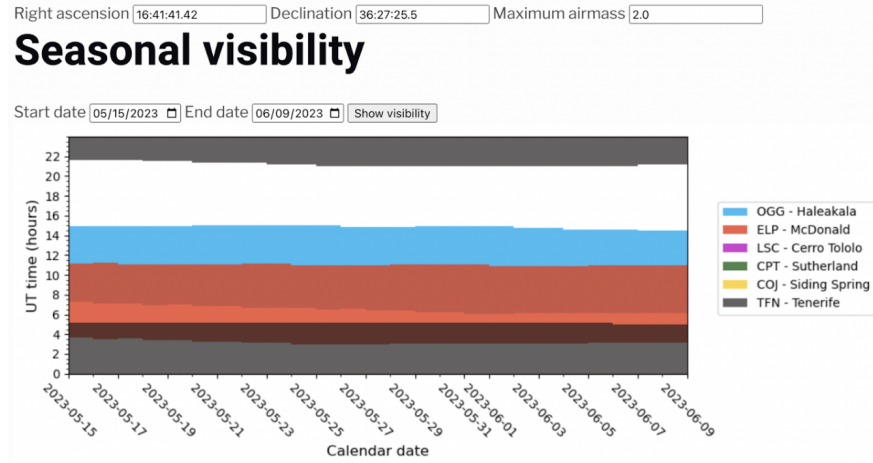


Figure 5: M13 visibility table. The colored lines represent the visibility at a given time from each telescope with the telescope of the corresponding color in the legend on the right.

We then submitted observation requests to Las Cumbres Observatory based on the visibility tables. Each star cluster was imaged for ten 15-second exposures in each filter (Sloan Digital Sky Survey Ultraviolet, Green, Red, and Infrared) for a total of 40 raw images per star cluster.

Each star cluster was imaged using LCO’s SBIG STL6303 0.4-meter telescope. The telescope is mounted in a 16-inch RCS tube, and it includes 3-element optics (primary, secondary, and corrector plate). Its corrector and secondary plates are driven by the LCO focus mechanism, and it has a tracking accuracy without guiding of approximately 1 arcsecond (*SBIG STL-6303*, n.d.). The SBIG STL6303 camera has a field of view of 29.2 arcminutes by 19.5 arcminutes, and its pixel scale is 0.571 with standard 1x1 binning. It has nine filter options, of which we chose four (*0.4-meter*, n.d.).

## 3.2 Composites

We created composites of all four filters for each exposure using Python. As seen in Figure 10, we set the file paths for each raw image, retrieved the data from each file, stacked the data, saved the composite .fit file, extracted the data, converted it to a 16-bit integer array, and then plotted and saved the image. This same process was repeated for all ten exposures of each star cluster. Next, we adjusted the light in AstroArt to complete the composite.



Figure 6: M44 SDSS i' filter



Figure 7: M44 SDSS r' filter



Figure 8: M44 SDSS g' filter

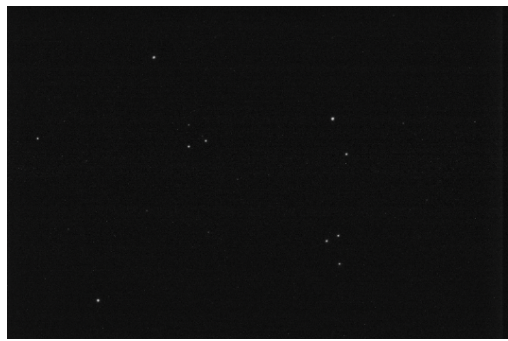


Figure 9: M44 SDSS u' filter



```

# stacking IRGB files
from astropy.io import fits
import numpy as np
import matplotlib.pyplot as plt

# set file paths
r_file = '/content/drive/MyDrive/Copy of tfn0m410-kb24-20230515-0063-e00.fits.fz' # exp 1
g_file = '/content/drive/MyDrive/Copy of tfn0m410-kb24-20230515-0053-e00.fits.fz'
b_file = '/content/drive/MyDrive/Copy of tfn0m410-kb24-20230515-0083-e00.fits.fz'
i_file = '/content/drive/MyDrive/Copy of tfn0m410-kb24-20230515-0073-e00.fits.fz'

# get the data from each .fits file
r_data, r_header = fits.getdata(r_file, header=True)
g_data, g_header = fits.getdata(g_file, header=True)
b_data, b_header = fits.getdata(b_file, header=True)
i_data, i_header = fits.getdata(i_file, header=True)

# stack the data from the .fits files
rgbi_array = np.stack((i_data, r_data, g_data, b_data), axis=-1)
rgbi_array = (rgbi_array - np.min(rgbi_array)) / (np.max(rgbi_array) - np.min(rgbi_array)) * 65535.0
rgbi_array = rgbi_array.astype(np.uint16)

# save the composite .fit file
fits.writeto('irgb_stacked_16bit.fit', rgbi_array, header=r_header, overwrite=True)

# Open the FITS file
hdulist = fits.open('irgb_stacked_16bit.fit')

# Extract the data
data = hdulist[0].data

# Convert the data to a 16-bit integer array
data_16bit = np.array(data, dtype=np.uint16)

# Plot and save image
plt.imshow(data_16bit, cmap='gray', vmin=0, vmax=2*16-1)
plt.axis('off')
plt.savefig('m13_irgb_exp1.jpg', dpi=300, bbox_inches='tight')

```

Figure 10: Compiling composites of each exposure for each star cluster in Python. This example displays the code for exposure 1 of M13.

### 3.3 HR Diagrams

To create the HR diagrams for each star cluster, we first liberated the .fits.fz files in Fits Liberator, converting them to .fits files. We then used Python to retrieve data from the .fits files, flatten the data, calculate the color index and absolute magnitude, plot the HR diagram for each exposure, and average all the HR diagrams. We calculated the color index by subtracting the g' filter flux data from the u' filter flux data and subtracting the r' filter flux data from the g' filter flux data. We created the HR diagrams by plotting each color index (u-g and g-r) against absolute magnitude for each exposure. Figures 11 and 12 show the Python code used to create and average the HR plots.



```

import numpy as np
import matplotlib.pyplot as plt
from astropy.io import fits

# Read the FITS files
r_data = fits.getdata('fn073_mol36_expl_filterrrp.fits.fits')
g_data = fits.getdata('fn053_mol34_expl_filtergrrp.fits.fits')
u_data = fits.getdata('fn083_mol37_expl_filterup.fits.fits')
i_data = fits.getdata('fn063_mol35_expl_filterrip.fits.fits')

# Flatten the data arrays
r_flux = -2.5*np.log10(r_data.flatten())
g_flux = -2.5*np.log10(g_data.flatten())
u_flux = -2.5*np.log10(u_data.flatten())
i_flux = -2.5*np.log10(i_data.flatten())

# Calculate the color index
U_V1 = u_flux - g_flux
V_R1 = g_flux - r_flux

# Calculate the absolute magnitude
abs_magnitude1 = i_flux - 2.5 * np.log10(1000) # Assuming a distance of 1000 parsecs

# Plot the HR diagram
plt.scatter(U_V1, abs_magnitude1, s=1, c='black')
plt.gca().invert_yaxis()
plt.xlabel('Color Index (u-g)')
plt.ylabel('Absolute Magnitude (i)')
plt.title('HR Diagram for Exposure 1')
plt.xlim(0.4, 1.6)
plt.grid(True)
plt.show()

# Plot the HR diagram
plt.scatter(V_R1, abs_magnitude1, s=1, c='black')
plt.gca().invert_yaxis()
plt.xlabel('Color Index (g-r)')
plt.xlim(.5, 1.5)
plt.ylabel('Absolute Magnitude (i)')
plt.title('HR Diagram for Exposure 1')
plt.grid(True)
plt.show()

```

Figure 11: Plotting HR diagrams of each exposure for each star cluster. This example displays the code for exposure 1 of M13.

To calculate absolute magnitude, we used data from the SDSS Infrared filter and the equation:

$$M_{abs} = m - 2.5 \log (ADU)$$

In this case, ADU (analog-to-digital units) = 1000, and m is given by:

$$m = -2.5 \log \left( \frac{peak\ density}{detection\ threshold} \right)$$

```

ave_U_V = np.mean([U_V1,U_V3,U_V4,U_V5,U_V6,U_V7,U_V8,U_V9,U_V10], axis = 0)
ave_absmag = np.mean([abs_magnitude1,abs_magnitude3,abs_magnitude4,abs_magnitude5, abs_magnitude6,
                      abs_magnitude7,abs_magnitude8,abs_magnitude9,abs_magnitude10], axis = 0)
ave_V_R = np.mean([V_R1,V_R3,V_R4,V_R5,V_R6,V_R7,V_R8,V_R9,V_R10], axis = 0)

plt.scatter(ave_U_V, ave_absmag, s=1, c='black')
plt.gca().invert_yaxis()
plt.xlabel('Color Index (u-g)')
plt.ylabel('Absolute Magnitude (i)')
plt.title('Averaged HR Diagram for all 10 Exposures of M13 ')
plt.xlim(0.25,1.7)
plt.grid(True)
plt.show()

plt.scatter(ave_V_R, ave_absmag, s=1, c='black')
plt.gca().invert_yaxis()
plt.xlabel('Color Index (v-r)')
plt.xlim(0.15, 1.25)
plt.ylabel('Absolute Magnitude (i)')
plt.title('Averaged HR Diagram for all 10 Exposures of M13 ')
plt.grid(True)
plt.show()

```

Figure 12: Averaging HR diagrams of each exposure to create compiled plots. This example shows M13’s code.

### 3.4 Signal to Noise Ratio

To compute the signal to noise ratio, we found the magnitude of twelve manually selected stars in each cluster using AstroArt and calculated the signal to noise ratio (SNR) using LCO’s exposure calculator (*Las Cumbres Observatory Exposure Time Calculator*, n.d.). We used the exposure 5 green filter raw image for each star cluster because the electromagnetic radiation of each cluster peaks in the green filter wavelength range (472 - 552 nm) (*Filters*, n.d.). In AstroArt, we selected one reference star using the Star Atlas tool, then manually selected eleven other stars. After running Photometry (Tools > Photometry), we retrieved the magnitude data of each star from AstroArt (View > Stars). We then input each magnitude (along with the telescope, filter, moon phase, and airmass) into LCO’s exposure calculator to find each star’s SNR.

We used the magnitude and SNR data to plot a log-scale graph of magnitude vs. SNR for each cluster in Python. As shown in Figure 13, we input the data into arrays, took the log of the magnitude data, found the line of best fit using np.polyfit, and plotted log(magnitude) against SNR with a line of best fit.

The equation to calculate the signal to noise ratio is as follows:

$$\frac{S}{N} = \frac{F A \epsilon Q_e \tau}{\sqrt{N_R^2 + \tau((F A \epsilon Q_e) + i_{DC} + F_\beta(A \epsilon Q_e) \Omega)}}$$

where  $F$  = point source signal flux on telescope (photon/s/cm<sup>2</sup>),  $A$  = telescope area (cm<sup>2</sup>),  $\epsilon$  = telescope efficiency,  $Q_e$  = quantum efficiency,  $\tau$  = integration time (s),  $N_R$  = read-out noise ( $e^-$ ),  $i_{DC}$  = dark current ( $e^-$ /s)  $F_\beta$  = background flux from sky (photons/s/cm<sup>2</sup>/arcsec<sup>2</sup>), and  $\Omega$  = pixel size (arcsec).

```
import numpy as np
import matplotlib.pyplot as plt
from matplotlib import rc

x = np.array([10.496, 11.733, 11.741, 11.779, 11.944, 12.547, 12.552, 12.748, 12.933, 13.152, 13.346, 13.673])
y = np.array([452.5, 250.5, 249.5, 244.9, 225.8, 166.4, 166, 149.9, 135.8, 120.5, 108.1, 89.5])
# magnitude data from AstroArt
# SNR data from LCO calculator
xlog = np.log10(x)
curve = np.polyfit(xlog, y, 1)
print(curve)

rc('xtick', **{'direction' : 'in', 'top': True, 'minor.visible' : True}) # tick marks go in and adding minor ticks
rc('ytick', **{'direction' : 'in', 'right': True, 'minor.visible' : True})

plt.plot(xlog, -3050.71772092*xlog + 3527.74545233, color = "orange", label = "best fit")
plt.scatter(xlog, y)
plt.legend()
plt.xlabel('Magnitude (log)')
plt.ylabel('SNR')
plt.title('M44 Magnitude vs. Signal to Noise Ratio')

plt.show()
```

Figure 13: Computing SNR in Python. This example shows M44’s magnitudes and SNR values as found by AstroArt and the LCO exposure calculator.

## 4 Results

### 4.1 Composites

Figures 14 and 15 display our exposure 1 composites of M44 and M13, respectively. Analysis, suggestions for improvements, and future projects can be found in sections 4.4 and 5.1.

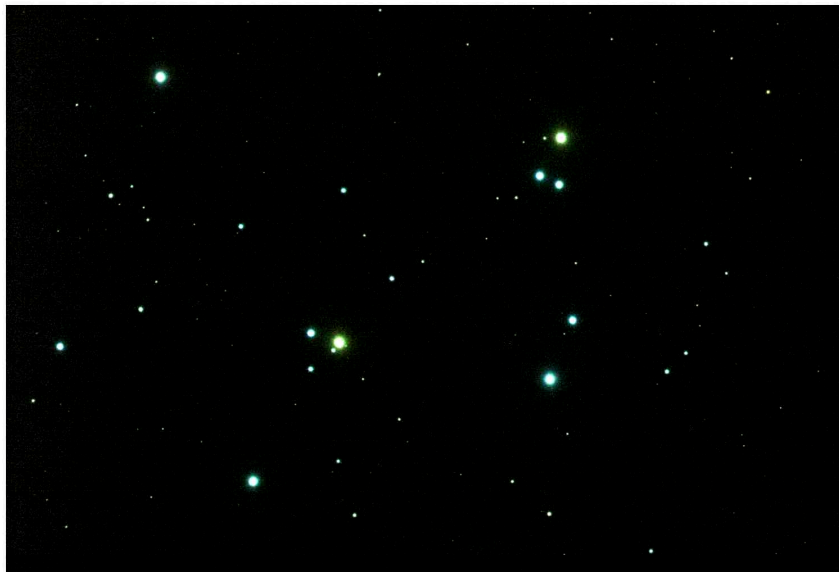


Figure 14: M44 Exposure 1 Color Composite



Figure 15: M13 Exposure 1 Color Composite

## 4.2 HR Diagrams

Figures 16 - 10 show our averaged HR diagrams for M44 and M13 with both the u-g and the g-r color index compared against professional HR diagrams for each cluster. Analysis and improvements can be found in sections 4.4 and 5.1.

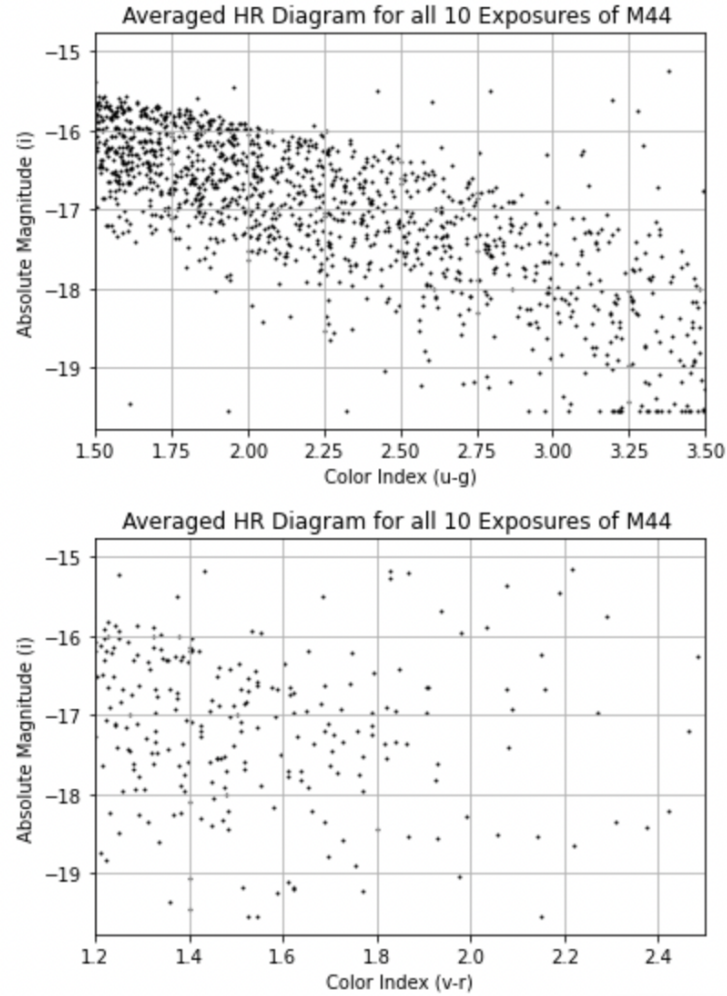


Figure 16: Our M44 HR diagrams

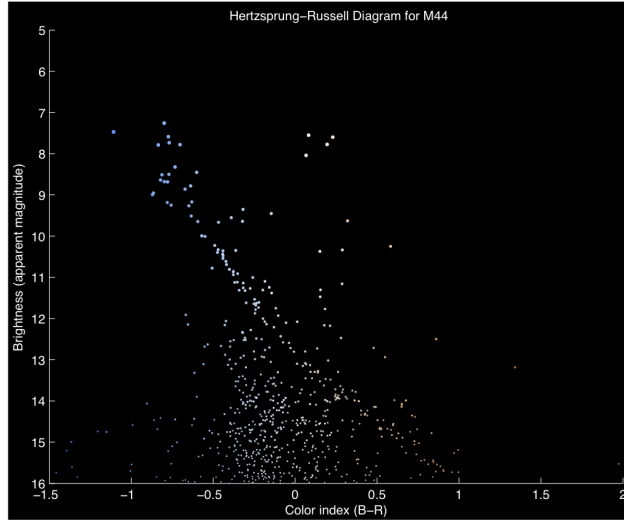


Figure 17: Professional M44 HR diagram (Vanderbei, n.d.)

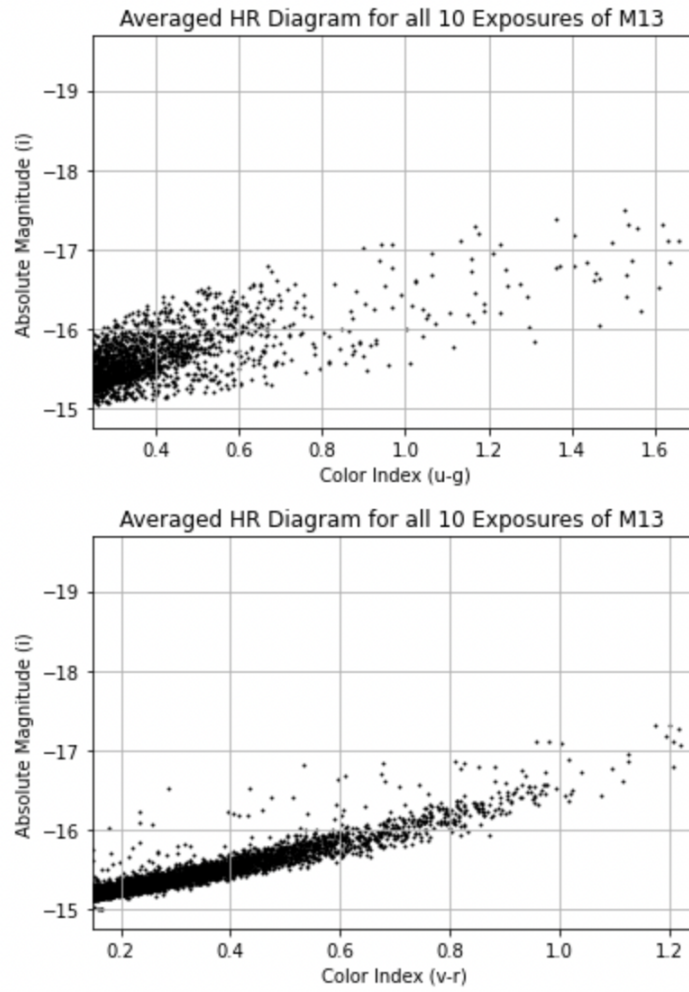


Figure 18: Our M13 HR diagrams



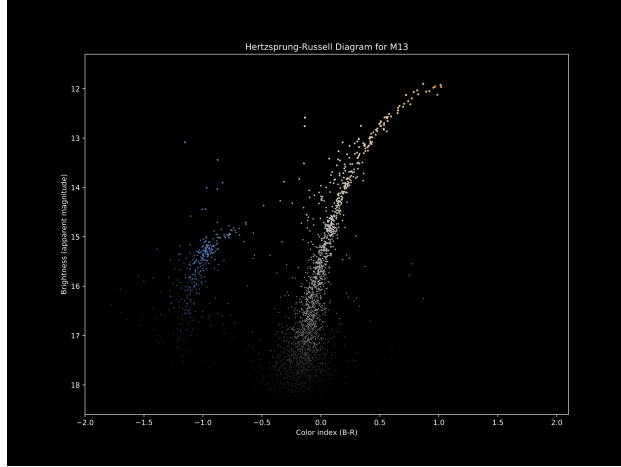


Figure 19: Professional M13 HR diagram (Vanderbei, n.d.)

### 4.3 Signal to Noise Ratio

The table below displays the magnitudes and SNR values of M44 and M13. Figures 20 and 21 show the log-scale graphs of these values with a best fit line.

Magnitude (M44)	SNR (M44)	Magnitude (M13)	SNR (M13)
10.496	452.4	11.379	297.4
11.733	250.5	11.733	250.5
11.741	249.5	12.746	150.0
11.779	244.9	13.016	129.8
11.944	225.8	13.363	107.1
12.547	166.4	13.537	97.5
12.552	166.0	13.563	95.5
12.748	149.9	13.750	85.5
12.933	135.8	13.875	79.3
13.152	120.5	13.878	79.1
13.346	108.1	13.930	76.7
13.673	89.5	13.978	74.4

[ -3050.71772092 3527.74545233 ]

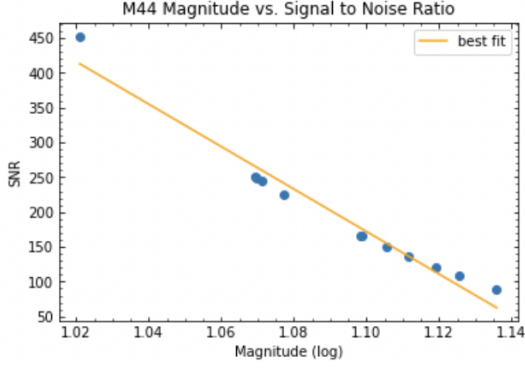


Figure 20: M44 Magnitude(log) vs. SNR

[ -2438.03432809 2858.9378158 ]

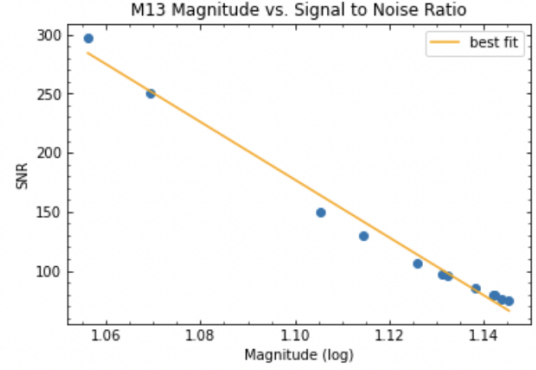


Figure 21: M13 Magnitude(log) vs. SNR

#### 4.4 Error

According to the European Southern Observatory, the relative error for SNR is  $1/SNR$ . The table below displays the error for each SNR value. M44's average relative error is 0.61%, and M13's average relative error is 0.96%.

SNR (M44)	Error (%) (M44)	SNR (M13)	Error (%) (M13)
452.4	0.22	297.4	0.33
250.5	0.40	250.5	0.40
249.5	0.40	150.0	0.67
244.9	0.41	129.8	0.77
225.8	0.44	107.1	0.93
166.4	0.60	97.5	1.0
166.0	0.60	95.5	1.0
149.9	0.67	85.5	1.2
135.8	0.74	79.3	1.3
120.5	0.83	79.1	1.3
108.1	0.93	76.7	1.3
89.5	1.1	74.4	1.3

Our primary systematic error was not aligning each image before making composites and HR diagrams. Since the images were not properly aligned using either AstroArt, astroalign,

or another alignment method, our HR diagrams (and to a lesser extent, our composites) are inaccurate. If we were to repeat the project, we would align the images before completing any further analysis. Additionally, had the images been aligned initially, it would have been easier to create a complete composite of all ten exposures for each star cluster.

Based on our signal to noise ratio values, we should have requested longer exposure times for M13. According to the European Southern Observatory, a SNR of 100 or over is ideal for measurement (Hainaut, n.d.), and according to the Las Cumbres Observatory, a SNR over approximately 455 (corresponding to a magnitude of 10.475 with our observing conditions) is susceptible to saturation (*Las Cumbres Observatory Exposure Time Calculator*, n.d.). Therefore, M13's SNR values (ranging from 74.4 to 297.4) should be increased for ideal measurement. The stars selected from M44, however, reach a maximum SNR of 452.2, which falls just below the threshold of saturation. If we were to repeat the project, we would have used the LCO exposure calculator before submitting observation requests to find an optimal exposure time for our desired SNR values.

## 5 Discussion

### 5.1 Implications

Our composite images confirm the age and density discrepancies between open clusters (M44) and globular clusters (M13). As seen in Figures 14 and 15, M44 is primarily composed of blue and green stars while M13 is made up of orange and red stars. Further, the averaged HR diagrams of M44 show a slight negative slope, which is the main sequence diagonal, and the averaged HR diagrams of M13 show a slight positive slope, which shows stars moving off of the main sequence toward the red giant phase of their lives. Since blue main sequence stars are younger than red giants, both the observed color and the HR diagram trends follow the trend noted in section 2.1: open clusters are younger than globular clusters. Additionally, both the composite image and the averaged HR diagrams for M44 display fewer, more diffuse stars than those of M13, which is accurate to preexisting information regarding the lower density of open clusters.

However, neither our composite images nor our HR diagrams show the younger, bluer stars that inhabit M13. Globular clusters often harbor multiple generations of stars, meaning that our M13 composite image should include blue stars in addition to the observed red stars and our M13 HR diagram should include main sequence stars in addition to the stars observed turning off the main sequence. Both of these observations can be seen in the professional composite and HR diagram of M13 (Figures 3 and 19). We hypothesize that a longer exposure time, aligning images, and creating a complete composite would result in a more accurate analysis of both star clusters, and M13's younger stars would be visible.

## **5.2 Limitations**

Our most significant limitations in this project were understanding and time. If we had time to submit another observation request with longer exposure times for M13 and fix our code by aligning the images or choosing reference stars in AstroArt to create the composites and HR diagrams, our results would have been much more accurate.

## **5.3 Conclusion**

Despite our inaccuracies, we gained valuable understanding and skills in astronomical observation and Python, and I am confident that a future project of a similar nature would be significantly more successful. Throughout the course of this project, we identified valid observation targets, submitted observation requests, compiled composites of each exposure, plotted averaged HR diagrams of all ten exposures for each star cluster, and computed signal to noise ratio for each cluster.

## References

- 0.4-meter*. (n.d.). Las Cumbres Observatory. Retrieved 06.11.2023, from <https://lco.global/observatory/telescopes/0m4/>
- Bolles, D. (2022). *M44: The Beehive Cluster*. Retrieved 06.11.2023, from <https://science.nasa.gov/m44-beehive-cluster>
- Evans, D. (2022). *M44: The Beehive Cluster*. Retrieved 06.11.2023, from <https://www.astrobin.com/c7c1x9/?q=M44%3A%20The%20Beehive%20Cluster%20Drew%20Evans>
- Filters*. (n.d.). Las Cumbres Observatory. Retrieved 06.11.2023, from <https://lco.global/observatory/instruments/filters/>
- Hainaut, O. (n.d.). *Signal, Noise and Detection*. Retrieved 06.11.2023, from <https://www.eso.org/~ohainaut/ccd/sn.html>
- Hertzsprung-Russell Diagram*. (n.d.-a). National Schools' Laboratory. Retrieved 06.11.2023, from <https://www.schoolsobservatory.org/learn/astro/stars/class/hrdiagram>
- The Hertzsprung-Russell Diagram*. (n.d.-b). Australia Telescope National Facility. Retrieved from <https://www.atnf.csiro.au/outreach/education/senior/astrophysics/stellarevolutionhrintro.html>
- Hertzsprung-Russell Diagram*. (2007). European Southern Observatory. Retrieved 06.11.2023, from <https://www.eso.org/public/images/eso0728c/>
- Las Cumbres Observatory Exposure Time Calculator*. (n.d.). Las Cumbres Observatory.
- Leach, S., & Block, A. (2008). *M13 Globular Star Cluster*. Retrieved 06.11.2023, from <http://www.sidleach.com/m13.htm>
- McClure, B., & Byrd, D. (2023). *The Beehive cluster: A swarm of 1,000 stars*. Retrieved 06.11.2023, from <https://earthsky.org/clusters-nebulae-galaxies/praesepe-beehive-cluster/>
- Miller, J. (2017). *Deep-Sky Objects: The Great Hercules Cluster (M13)*. Retrieved 06.11.2023, from <https://www.astronomytrek.com/deep-sky-objects-the-great-hercules-cluster-m13/>

Palma, C. (n.d.). *Measuring the Age of a Star Cluster*. Retrieved 06.11.2023, from <https://www.e-education.psu.edu/astro801/content/17p6.html>

Plotner, T. (n.d.). *Messier 13 (M13) – The Great Hercules Cluster*. Retrieved 06.11.2023, from <https://www.universetoday.com/31430/messier-13/>

*SBIG STL-6303*. (n.d.). Las Cumbres Observatory. Retrieved 06.11.2023, from <https://lco.global/observatory/instruments/sbig-stl-6303/>

*Star Clusters*. (n.d.). Harvard Smithsonian Center for Astrophysics. Retrieved 06.11.2023, from <https://www.cfa.harvard.edu/research/topic/star-clusters>

Vanderbei, R. J. (n.d.). *Hertzsprung-Russell Diagrams for Globular and Open Clusters*. Retrieved 06.11.2023, from <https://vanderbei.princeton.edu/images/NJP/HRdiag.html>

(*Hertzsprung-Russell Diagram*, n.d.-a) (Palma, n.d.) (Vanderbei, n.d.) (*The Hertzsprung-Russell Diagram*, n.d.-b) (*0.4-meter*, n.d.) (Leach & Block, 2008) (Miller, 2017) (Plotner, n.d.) (Evans, 2022) (McClure & Byrd, 2023) (Hainaut, n.d.) (*SBIG STL-6303*, n.d.) (*Star Clusters*, n.d.) (Bolles, 2022) (*Filters*, n.d.) (*Las Cumbres Observatory Exposure Time Calculator*, n.d.)